J Mater Sci (2022) 57:1536–1544

Polymers & biopolymers

Adsorption kinetics of gaseous chlorobenzene on electrospun lignin-based nanofiber

Yaxin Hu[1], Yue Zhou[1], Zhou Yang[2], Fang Ren[1], Zhennan Chen[1], Yixiao Fu[1], Ruoyu Dong[1], Liangbiao Wang[1], Quanfa Zhou[3,*], and Hengfei Qin[1,*]

[1] School of Chemistry and Environmental Engineering, Jiangsu University of Technology, Changzhou 213001, China
[2] Department of Material Engineering, Jiangsu University of Technology, Changzhou 213001, China
[3] Research Center of Secondary Resources and Environment, Changzhou Institute of Technology, No.666, Liaohe Road, Changzhou City 213022, China

Received: 21 August 2021
Accepted: 17 November 2021
Published online: 3 January 2022

ABSTRACT

In this paper, lignin-based nanofiber materials with excellent adsorption performance were prepared by electrospinning technology with waste lignin as raw material and doped Ni-MOF-74. Through a series of characterization of the adsorbent, the effects of fiber morphology, pore size distribution, and doping Ni-MOF-74 on chlorobenzene adsorption performance were studied. It showed that doping Ni-MOF-74 could effectively increase the specific surface area of the adsorbent, enrich the pore structure, which was conductive to the adsorption. The results showed that Ni-MOF-74 doped lignin fiber exhibits excellent chlorobenzene adsorption performance compared with Ni-MOF-74 material and lignin fiber, and the maximum adsorption capacity can reach 58.49 g/g. According to the calculation of Langmuir equation, the chemical adsorption plays a leading role in the adsorption process of chlorobenzene.

Introduction

Volatile organic compounds (VOCs) are air pollutants with toxic, irritating, teratogenic and carcinogenic effects [1–3]. Benzene series such as chlorobenzene are typical representatives of such pollutants, which mainly come from industrial waste gas, photochemical pollution, decorative paint, etc. [4, 5]. In recent years, the environmental pollution problem has become increasingly serious, and the effective management of VOCs has attracted extensive attention of many researchers.

VOCs treatment technology mainly includes adsorption, catalytic combustion and high temperature incineration technology, among which the adsorption method is a cost-effective treatment method because of its simple operation and excellent adsorption effect [6–15]. Adsorption is divided into physical adsorption and chemical adsorption, and the commonly used adsorbents mainly include silica gel,

Handling Editor: Stephen Eichhorn.

Address correspondence to E-mail: labzqf@czu.cn; jlgqinhf@jsut.edu.cn

https://doi.org/10.1007/s10853-021-06739-8

activated carbon, zeolite molecular sieve, etc. Li et al. using the multi-pores of activated carbon to provide channels for chlorobenzene, to achieve multi-layer physical adsorption, but its saturated adsorption capacity is only 178.3 mg/g [16]. Using P123 as structural guiding agent, Zhang et al. prepared micro-mesoporous UiO-66 by a simple solvothermal method. The material adsorbed toluene vapor mainly through micropores. Meanwhile, the large pores in micro-mesoporous UiO-66 increased the molecular diffusion rate, reduced the mass transfer resistance, and made the micropores better capture toluene molecules. The optimum saturated adsorption capacity is 394 mg/g [17]. But the defect of physical adsorption is that the adsorption stability is poor and the adsorbed gas is easy to desorption. Therefore, the preparation of chemisorption-based adsorbent materials with high efficiency and environmental protection has become one of the research hotspots.

In recent years, nanomaterials have been widely used in various fields, among which nanofiber can be used as a new adsorbent material for the treatment of VOCs. Main preparation methods of nanometer fiber include stretching, template polymerization, phase separation, self-organization and electrospinning; in particular, electrospinning has simple and controllable process flow, wide source of raw materials and low cost [18–20]. This method mainly regulates the ratio of raw materials to polymer compounds (PAN, PVP, PEO, etc.), voltage, jet speed, receiving distance and other parameters; thus, continuous nanofibers are prepared [21–23]. It should be noted that polymer compounds play a bonding role in the spinning solution, and its dosage will directly affect the preparation of continuous nanofibers.

In this paper, waste lignin was used as raw material and doped with Ni-MOF-74, so as to increase the specific surface area and enrich the pore structure [24]. Through electrospinning technology, lignin-based nanofiber dominated by chemical adsorption and combined with physical adsorption were prepared, which were applied to adsorb the pollutant chlorobenzine. Through a series of characterization of the adsorbent, the effects of fiber morphology, pore size distribution and doping Ni-MOF-74 on the adsorption performance were studied. Through the test of adsorption performance, the adsorption stability was studied, and compared with Ni-MOF-74 material and lignin fiber, the adsorbent with the best adsorption performance was obtained, and the adsorption mechanism was further explored by Langmuir equation.

Experimental

Lignin pretreatment

A certain amount of organic lignin were put into a beaker and placed in a mixture of ethyl acetate/ethyl ether (volume ratio: 2/1). The lignin was washed for several times, collected by centrifugation, and freeze-dried to prepare the lignin required for the experiment.

Preparation of Ni-MOF-74

A certain amount of nickel nitrate hexahydrate and 2,5-dihydroxyterephthalic acid (molar ratio: 10/1, mmol) were, respectively, weighed into a mixture of 60 mL N, N-dimethylformamide (DMF), 5 mL methanol and 5 mL deionized water, and then, the precursor solution of Ni-MOF-74 was prepared by stirring evenly. After stirring evenly, the material was placed in the TEflon hydrothermal reaction kettle for thermal reaction at 100 °C for 36 h. After cooling, the precipitation in the reactor was collected, washed with methanol for several times, centrifuged to collect the precipitation in the tube, and freeze-dried to obtain Ni-MOF-74 material.

Electrospun lignin fiber

In a typical procedure, the weight ratio of lignin/ PEO/ Ni-MOF-74 was set to 4.5/ 1/ 0.01, then dissolved in an appropriate amount of DMF, heated and stirred at 40 °C for 24 h. Before spinning, the spinning solution was ultrasonically broken for 20 s, and the electrospinning equipment was preheated at 30 °C. The aluminum foil paper was prepared and placed on the receiver, the 5 mL syringe equipped with 22G needle is used as the spinner, and the parameters such as voltage, injection speed and receiving distance were adjusted. When the stable "Taylor cone" was formed in front of the needle, the equipment door could be closed, and the spinning time was about 6 ~ 7 h. The obtained lignin fiber was labeled as L/P/Ni-4.5. As in the above steps, the weight ratio of lignin/PEO/Ni-MOF-74 was set to 4.2/1/0.01 and 4/1/0.01 labeled as L/P/

Ni-4.2 and L/P/Ni-4. Lignin fibers were electrospun without Ni-MOF as a reference. The specific spinning setting parameters are shown in Table 1.

Materials characterization and adsorption evaluate

Physical and chemical properties of the obtained materials were analyzed by field-emission scanning electron microscope (FE-SEM, Sigma 500) including element mapping and transmission electron microscopy (TEM, JEM-2100). N_2 adsorption–desorption isotherms were measured at − 196 °C on an automated volumetric apparatus NOVA2000e (Quantachrome Instruments, USA). About 10 mL chlorobenzene were put into a closed jar and heated in a water bath at 40 °C to evaporate into chlorobenzene. Then, the Ni-MOF-74, lignin fiber, L/P/Ni-4.2 and L/P/Ni-4 fiber were placed in the jar respectively to adsorb chlorobenzene. Weigh the sample every half an hour until the weight was constant. After the adsorption reaction, the sample with the best adsorption performance was desorbed and readsorbed in a cycle until the final adsorption rate fluctuates within a certain range. In addition, in order to verify whether the adsorption capacity can be effectively increased by doping Ni-MOF-74, the primary saturated adsorption capacity of the above samples and single component lignin and PEO were repeated three times.

Results and discussion

It can be seen from Fig. 1a, b that when the ratio of lignin to PEO is 4.5:1, the L/P/Ni-4.5 fiber exists in the form of rod and is discontinuous. The spinning solution sprayed from the needle tip during electrospinning is linear and cannot form a complete "Taylor cone." The reason for this phenomenon may be that the lignin content is too high and the chemical crosslinking with PEO is poor, which makes it impossible to spin. Compared with L/P/Ni-4.5, when the ratio of lignin to PEO is 4.2:1, the L/P/Ni -4.2 fiber (Fig. 1c, d) presents a smooth filamentous surface, with a length of about 5–10 μm and a diameter of 80–120 nm. The spinning performance is improved, but it is still discontinuous and broken.

The field-emission scanning electron microscopy (FE-SEM) in combination with energy-dispersive spectrometer (EDS) mapping images display the morphology of L/P/Ni-4 as shown in Fig. 2. As shown in Fig. 2a–d, when the ratio of lignin to PEO is 4:1, continuous nanofibers with uniform diameter distribution, non-fracture and long-range order can be prepared, which can form a three-dimensional network structure and provide more adsorption binding sites. From the element mapping of L/P/Ni-4 (Fig. 2e–f), the fiber contains elements C, Ni, O, which indicates the Ni-MOF-74 can be successfully loaded on the fiber.

Nitrogen adsorption–desorption isotherms and pore size distribution curves are presented in Fig. 3. As can be seen from Fig. 3a, the adsorption and desorption isotherm of Ni-MOF-74 shows a small adsorption increment with the increase in relative pressure, only when the relative pressure is between 0.01 and 0.5, there is a steep and large adsorption, and the curve presents an approximate horizontal platform on the whole, indicating that the pore size distribution range of Ni-MOF-74 is narrow and mainly exists in the form of micropores. The adsorption hysteresis of Ni-MOF-74 shows hysteresis ring, which indicates that Ni-MOF-74 has a small number of mesoporous and conforms to the characteristics of type IV isotherm. The adsorption and desorption isotherms of lignin fiber and L/P/Ni-4 are convex at a higher relative pressure, and there is a hysteresis loop when their relative pressures are between 0.6 and 0.9 [25, 26], indicating that there are

Table 1 Setting parameters of electrospinning

Injection speed (mm/min)	Positive voltage (Kv)	Negative voltage (Kv)	Reception speed (r/min)
0.08	10 ~ 11	− 1.5 ~ − 2.5	60
Receiving distance(cm)	Translational velocity(mm/min)	Temperature (°C)	Humidity (%)
12 ~ 13	55	30 ~ 32	32 ~ 40

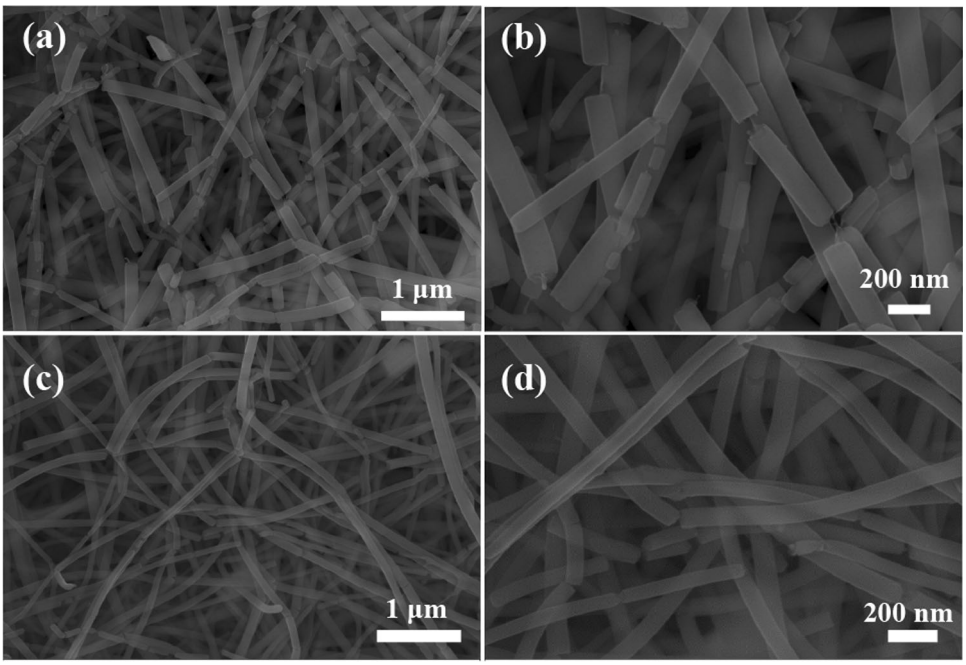

Figure 1 **a**, **b** FE-SEM images of L/P/Ni-4.5 and **c**, **d** SEM image of L/P/Ni-4.2.

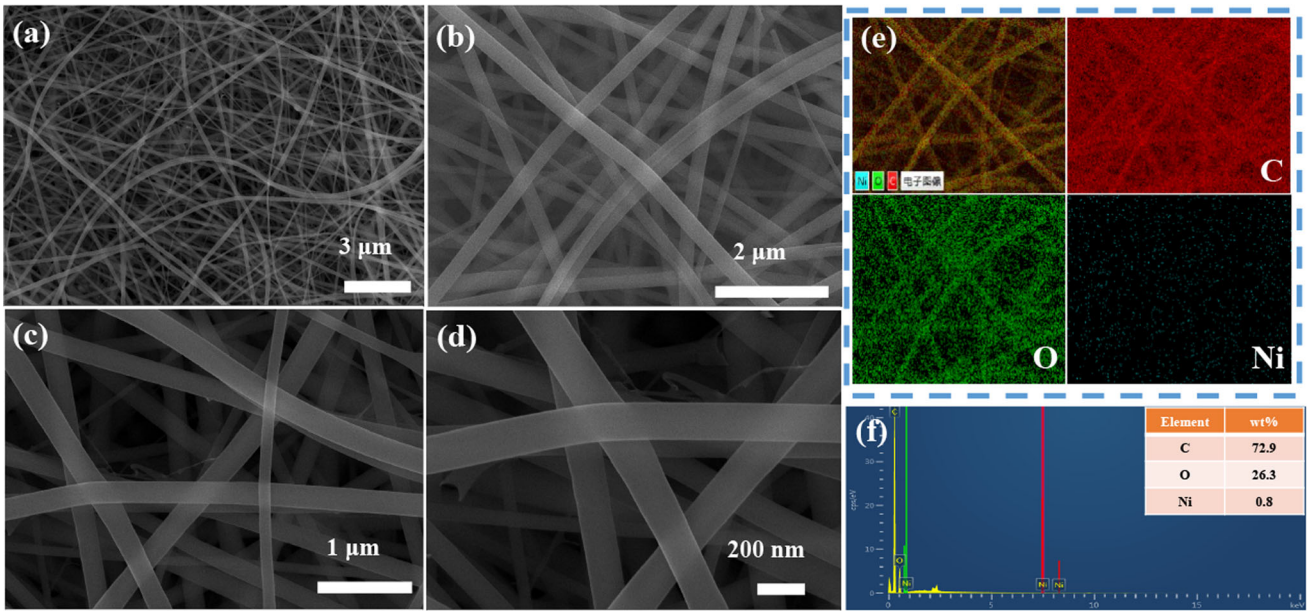

Figure 2 **a** ∼ **d** SEM image and **e** ∼ **f** EDS mapping images of L/P/Ni-4.

a large number of mesopores in the lignin fiber and L/P/Ni-4.

As can be seen from Fig. 3b, the pore size distribution curves show that the pore size of Ni-MOF-74 exists in the form of micropores and mesopores, but most of them are micropores. The pore size of lignin fiber exists in the form of mesoporous; however, L/P/Ni-4 exists in the form of micropores and mesopores, and most of them are mesopores, which is consistent with the conclusion obtained from the adsorption and desorption isotherm. It can be inferred that doped Ni-MOF-74 enriches the pore structure, mesopores provide adsorption and desorption channels to improve the adsorption and diffusion rate; meanwhile, micropores can further anchor chlorobenzene molecules and improve the adsorption capacity [17]. Since the specific surface area and pore volume of Ni-MOF-74 are large, doping Ni-

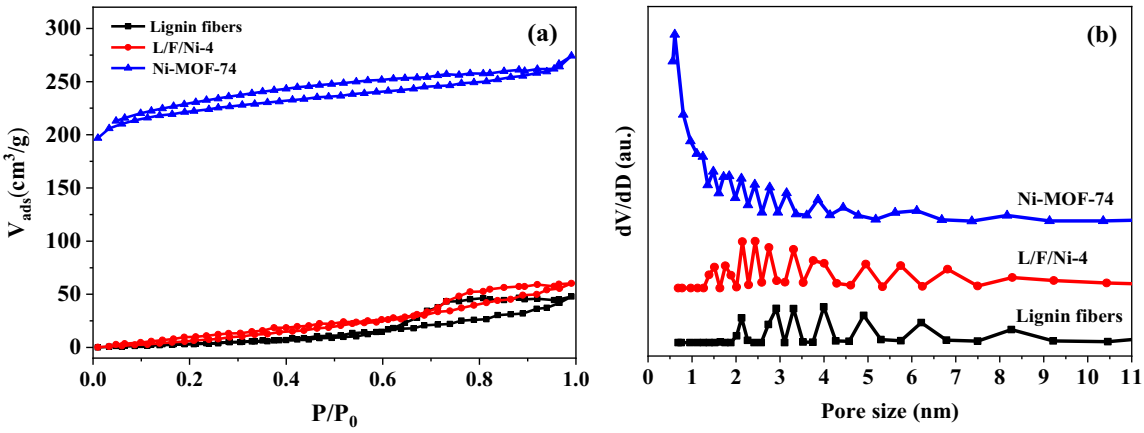

Figure 3 **a** N_2 sorption isotherms and **b** pore size distribution curves of lignin fibers, L/P/Ni-4 and Ni-MOF-74.

MOF-74 can make the specific surface area of L/P/Ni-4 significantly larger than that of lignin fiber and also make the pore volume of L/P/Ni-4 slightly larger than that of lignin fiber, which is conducive to improving the adsorption capacity. The specific surface area and pore volume of the samples are shown in Table 2.

Figure 4 shows the comparison of sample properties for the adsorption of gaseous chlorobenzene. As can be seen from Fig. 4, the L/P/Ni-4 showed excellent adsorption performance for chlorobenzene, which was higher than all of other samples. Compared with the adsorption capacity of lignin-based fiber, the adsorption capacity of Ni-MOF-74 is very low. It can be inferred that although the specific surface area of Ni-MOF-74 is large, its micropore size is close to the molecular diameter of chlorobenzene (0.6 ~ 0.7 nm), and even a small amount of micropore size is smaller than the molecular diameter of chlorobenzene. In addition, Ni-MOF-74 is an inorganic substance while chlorobenzene is an organic substance, and there is an interface effect between them, which will lead to a low adsorption capacity. In order to further study which substance is the main contributor to the adsorption of chlorobenzene, the adsorption properties of PEO and lignin for chlorobenzene were also studied. As can be seen from Fig. 4a, it is easy to find that the adsorption capacity of lignin and Ni-MOF-74 for chlorobenzene is basically the same, and the adsorption capacity of both is twice that of PEO.

Furthermore, comparing the adsorption capacity of L/P/Ni-4 and L/P/Ni-4.2, it can be seen that the adsorption capacity of L/P/Ni-4.2 was much smaller than that of L/P/Ni-4, and the increase trend of adsorption capacity was gentle. When the ratio of lignin to PEO is 4.2:1, the fiber breaks, which is not conducive to the formation of p-π conjugate bond between the O atom on the aryl ether bond of lignin and the benzene ring on chlorobenzene, resulting in the greatly weakened adsorption performance. It can be inferred that the surface functional groups of lignin play a leading role in the adsorption of chlorobenzene. The saturated adsorption capacity of all samples is shown in Fig. 4b. The saturated adsorption capacity of L/P/Ni-4, lignin fibers, L/P/Ni-4.2, lignin, Ni-MOF-74 and PEO for chlorobenzene is 58.49, 42.34, 7.95, 4.03, 3.93 and 2.14 g/g, respectively. Moreover, the error bars in Fig. 4b indicate that doping Ni-MOF-74 can effectively improve the adsorption capacity.

In this paper, the Langmuir equation was used to describe the adsorption behavior of chlorobenzene vapor on L/P/Ni-4 fiber. The fitting curve and related parameters of Langmuir equation are shown in Fig. 5 and Table 3, respectively. The results show that the pseudo-second-order kinetic model of L/P/Ni-4 has a higher fitting correlation, R^2 can reach 0.987, and the equilibrium adsorption capacity obtained by the pseudo-second-order kinetic model is closer to the actual value (58.49 g/g). Therefore, the

Table 2 Specific surface area and pore volume of the samples

Sample	Surface area (m^2/g)	Pore volume (cc/g)
Lignin fiber	33.949	0.090
L/P/Ni-4	81.617	0.118
Ni-MOF-74	874.415	0.190

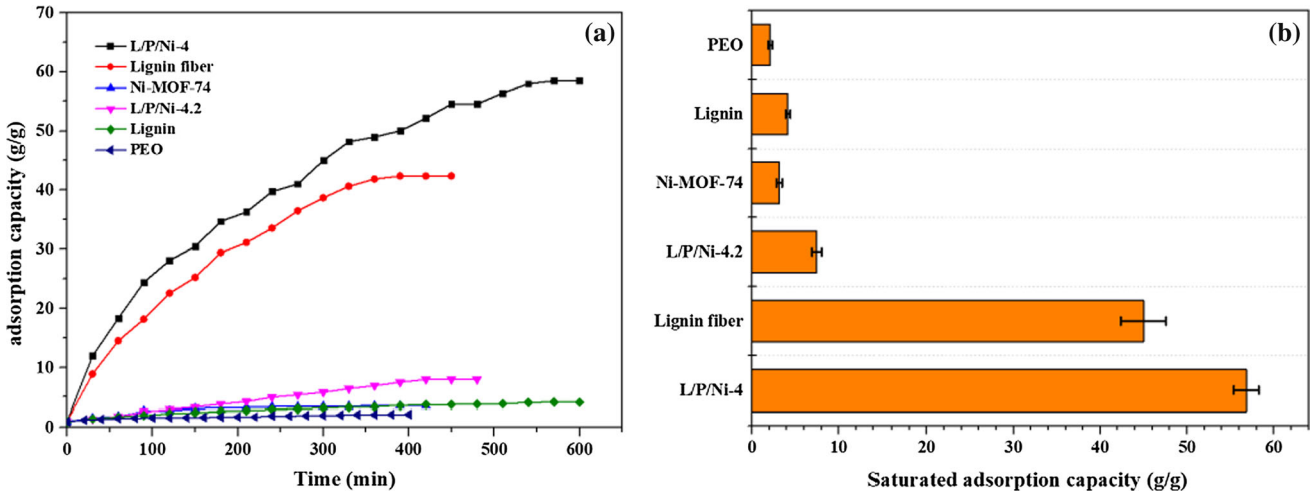

Figure 4 The adsorption and saturated adsorption capacity of gaseous chlorobenzene for all of the samples.

adsorption of chlorobenzene by L/P/Ni-4 conforms to pseudo-second-order kinetic model, and chemisorption plays a leading role.

In the adsorption process, physical adsorption plays a complementary role, chlorobenzene molecules diffused into the pore, which can be analyzed by using the intra-particle diffusion model. It can be seen from Fig. 6a and Table 4 that the adsorption capacity of chlorobenzene by L/P/Ni-4 increase rapidly from 0 to 48.177 g/g in the first 330 min. With the passage of adsorption time, the chlorobenzene molecules gradually move from the mesopore to the micropore, and the adsorption rate in the micropore decrease. The adsorption capacity of L/P/Ni-4 for chlorobenzene tend to be flat after 330 min, and the adsorption of chlorobenzene by L/P/Ni-4 basically reached equilibrium.

Recyclability is an important index to investigate the performance of adsorbent. In this paper, the desorption and readsorption of L/P/Ni-4 are carried out. After six cycles of adsorption, the adsorption capacity fluctuates between 9.6 and 11 g/g. As can be seen in Fig. 6b, the initial adsorption of chlorobenzene by L/P/Ni-4 is extremely high, and then, the adsorption capacity decreases significantly. Since L/P/Ni-4 is a chemisorption adsorbent, and the electrospinning technology makes the O atoms on the aryl ether bond of lignin more strongly bind to the benzene ring of chlorobenzene, it is difficult to fully desorption chlorobenzene during the desorption process, resulting in the decline of the adsorption capacity of L/P/Ni-4. But its final saturated adsorption capacity is still up to about 10 g/g, which is much higher than that of adsorbents dominated by physical adsorption, such as activated carbon, molecular sieve and other materials.

According to the above analysis, a schematic diagram of chlorobenzine adsorption mechanism over

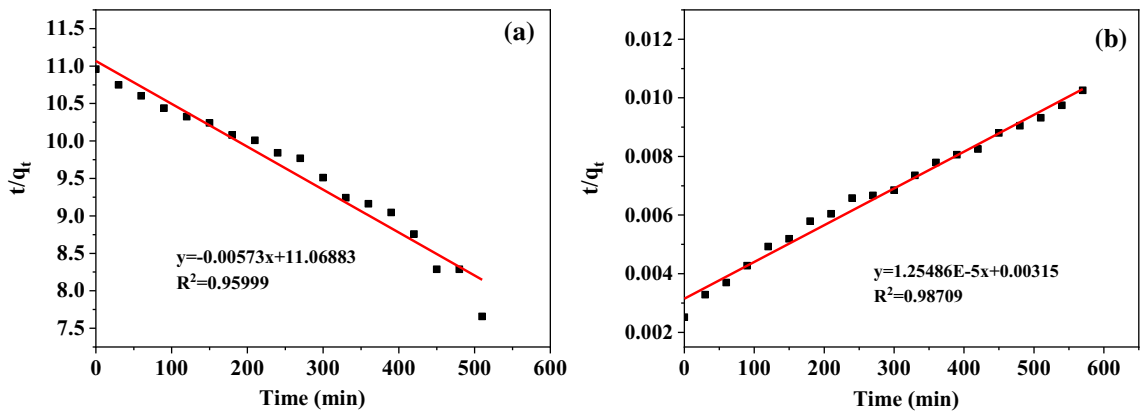

Figure 5 Adsorption kinetics fitting curve of L/P/Ni-4: **a** Pseudo-first-order, **b** Pseudo-second-order.

Table 3 Kinetic parameters of L/P/Ni-4

Sample	Pseudo-first-order			Pseudo-second-order		
	$q_{e,1}$	k_1	R^2	$q_{e,2}$	k_2	R^2
L/P/Ni-4	58.556	0.00573	0.95999	58.494	1.25×10^{-5}	0.98709

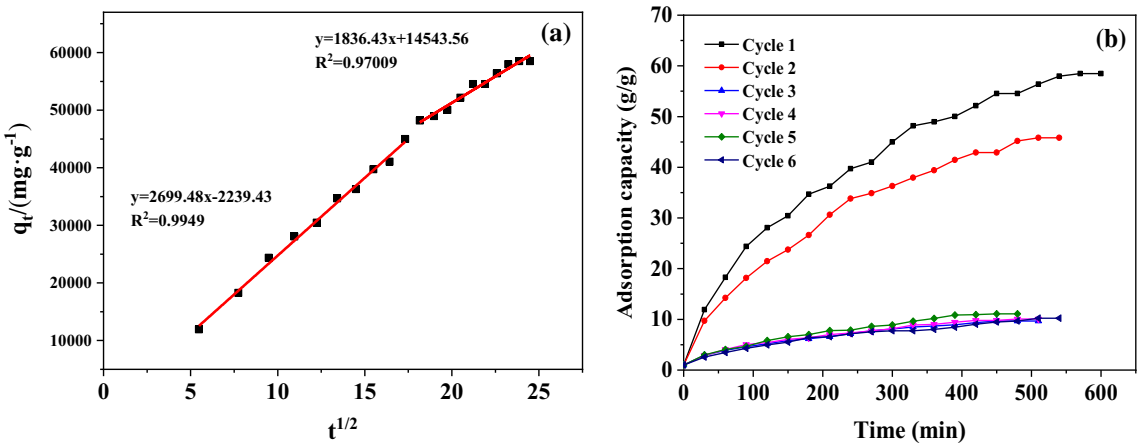

Figure 6 **a** The fitting curve of the in-particle diffusion and **b** cycle running of chlorobenzene adsorption over the L/P/Ni-4.

Table 4 The parameters of the in-particle diffusion model for L/P/Ni-4

Sample	$K_{3,1}$	L_1	R_1^2	$K_{3,2}$	L_2	R_2^2
L/P/Ni-4	2699.48	2239.43	0.9949	1836.43	14,543.56	0.97009

L/P/Ni-4 is shown in Fig. 7. In general, first, L/P/Ni-4 is made by electrospinning to form a three-dimensional network of fibers that can be used to wrap chlorobenzene molecules. Secondly, the addition of Ni-MOF-74 to the spinning solution makes the fiber have larger specific surface area and richer pore structure, and the microporous structure can also further anchor chlorobenzene molecules, resulting in a synergistic effect, showing excellent physical adsorption capacity. According to the adsorption experiment, the adsorption capacity of L/P/Ni-4 is very high, but the adsorption capacity of its single component is opposite. Therefore, the adsorption capacity of L/P/Ni-4 is not due to the simple superposition of single components, but to the chemical binding between L/P/Ni-4 and chlorobenzene. The Langmuir equation calculation also shows that L/P/Ni-4 is a chemisorption adsorbent. As can be seen from Fig. 7, the O atoms on the aryl ether bond of lignin provide lone electron pairs and form p-π conjugation system with the benzene ring on the chlorobenzine [27], which makes the chlorobenzene molecules adsorbed on L/P/Ni-4 firmly.

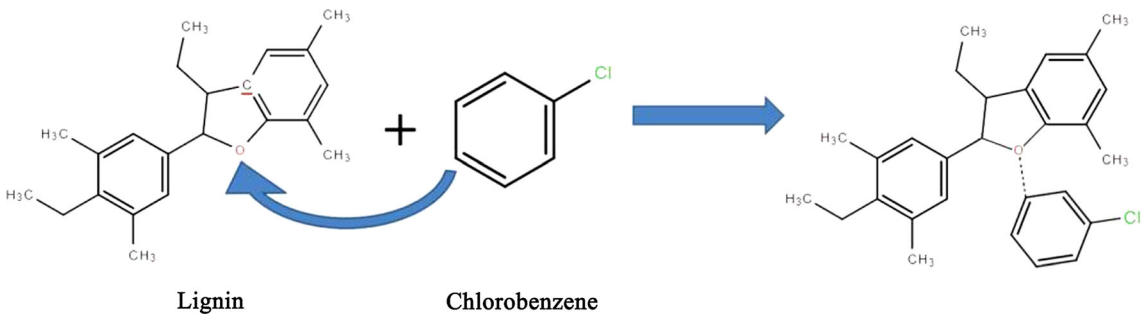

Figure 7 A plausible adsorption mechanism of chlorobenzine on L/P/Ni-4.

Conclusions

In summary, L/P/Ni-4 was prepared by electrospinning, and its morphology is continuous nanofibers with uniform diameter distribution. The micro-mesoporous structure of the material can anchor chlorobenzene molecules and effectively improve the adsorption capacity. By studying the effect of the ratio of lignin to PEO on the morphology and adsorption properties of the fiber, it can be concluded that when the ratio of lignin to PEO is 4.2:1, the fiber breaks and the adsorption capacity is low due to the insufficient amount of PEO; when the ratio of lignin to PEO is 4:1, the prepared continuous nanofibers can provide more adsorption binding sites, so that the O atom on the aryl ether bond of lignin provides lone pair electron pairs, and forms more p-π conjugated systems with the benzene ring on chlorobenzene, so as to further improve the adsorption capacity. According to the calculation of Langmuir equation, L/P/Ni-4 is an adsorbent dominated by chemical adsorption, and after multiple adsorption, the adsorption capacity remains stable at about 10 g/g, showing the reusability of the adsorbent. The excellent adsorption performance, material reusability and environmental protection provide the possibility for the practical application of L/P/Ni-4 in this paper.

Acknowledgements

This work was supported by the National Natural Science Foundation of China (Grant No. 31800495), Natural Science Foundation of Jiangsu Province (BK20181040) and China Postdoctoral Science Foundation (2019M653654). National key research and development project (Grant No. 2018YFC1902503-2). We are grateful for financial support from Qing Lan Project of Jiangsu Province.

References

[1] Shi X, Zhang X, Bi F et al (2020) Effective toluene adsorption over defective UiO-66-NH_2: an experimental and computational exploration. J Mol Liq 316:113812

[2] Qin H, Jin JL, Zheng PH et al (2009) Dynamic adsorption of volatile organic compounds on organofunctionalized SBA-15 materials. Chem Eng J 149(1–3):281–288

[3] Zhang G, Feizbakhshan M, Zheng S et al (2019) Effects of properties of minerals adsorbents for the adsorption and desorption of volatile organic compounds (VOC). Appl Clay Sci 173(JUN):88–96

[4] Zhang X, Yang Y, Song L et al (2018) Enhanced adsorption performance of gaseous toluene on defective UiO-66 metal organic framework: Equilibrium and kinetic studies. J Hazard Mater 365(MAR.5):597–605

[5] Yang L, Jing L, Lu B et al (2010) Study on the removal of indoor VOCs using biotechnology. J Hazard Mater 182(1–3):204–209

[6] Zhang XD, Wang Y, Yang YQ et al (2015) Recent progress in the removal of volatile organic compounds by mesoporous silica materials and supported catalysts. Acta Phys Chim Sin 31(9):1633–1646

[7] Lillo-Ródenas MA, Fletcher AJ, Thomas KM et al (2006) Competitive adsorption of a benzene-toluene mixture on activated carbon at low concentration. Carbon 44(8):1455–1463

[8] Zhang XD, Xu T et al (2018) Enhanced hydrophobic UiO-66 (University of Oslo 66) metal-organic framework with high capacity and selectivity for toluene capture from high humid air. J Colloid Interface Sci 539:152–160

[9] Guo Y, Li Y, Wang J et al (2014) Effects of activated carbon properties on chlorobenzene adsorption and adsorption product analysis. Chem Eng J 236:506–512

[10] Dobre T, Parvulescu OC, Iavorschi G et al (2014) Volatile organic compounds removal from gas streams by adsorption onto activated carbon. Ind Eng Chem Res 53(9):3622–3628

[11] Asnin LD, Davankov VA, Pastukhov AV (2008) The adsorption of chlorobenzene on a carbon adsorbent obtained by the pyrolysis of hypercrosslinked polystyrene. Russ J Phys Chem A 82(13):2313–2317

[12] Gironi F, Piemonte V (2011) VOCs removal from dilute vapour streams by adsorption onto activated carbon. Chem Eng J 172(2–3):671–677

[13] Lin L, Liu S, Liu J (2011) Surface modification of coconut shell based activated carbon for the improvement of hydrophobic VOC removal. J Hazard Mater 192(2):683–690

[14] Savita KPV, De Geyter N, Giraudon JM et al (2019) The use of zeolites for VOCs abatement by combining non-thermal plasma, adsorption, and/or catalysis: a review. Catalysts 9(1):98

[15] Gaur V, Asthana R, Verma N (2006) Removal of SO_2 by activated carbon fibers in the presence of O_2 and H_2O. Carbon 44(1):46–60

[16] Li Y, Guo Y, Zhu T et al (2016) Adsorption and desorption of SO_2, NO and chlorobenzene on activated carbon. J Environ Sci 043(005):128–135

[17] Zhang X, Yang Y, Lv X et al (2019) Adsorption/desorption kinetics and breakthrough of gaseous toluene for modified microporous-mesoporous UiO-66 metal organic framework. J Hazard Mater 366:140–150

[18] Ago M, Okajima K, Jakes JE et al (2012) Lignin-based electrospun nanofibers reinforced with cellulose nanocrystals. Biomacromol 13(3):918–926

[19] Cho MJ, Karaaslan MA, Renneckar S et al (2017) Enhancement of the mechanical properties of electrospun lignin-based nanofibers by heat treatment. J Mater Sci 52(16):1–13. https://doi.org/10.1007/s10853-017-1160-0

[20] Qin H, Zhou Y, Bai J et al (2017) Lignin-derived thin-walled graphitic carbon-encapsulated iron nanoparticles: growth, characterization, and applications. ACS Sustain Chem Eng 5(2):1917–1923

[21] Cho MJ, Ko FK, Renneckar S (2019) Impact of thermal oxidative stabilization on the performance of lignin-based carbon nanofiber mats. ACS Omega 4(3):5345–5355

[22] Cho MJ, Ji L, Liu LY et al (2020) High performance electrospun carbon nanofiber mats derived from flax lignin. Ind Crops Prod 155:112833

[23] Xiong F, Han Y et al (2017) Preparation and formation mechanism of renewable lignin hollow nanospheres with a single hole by self-assembly. ACS Sustain Chem Eng 5(3):2273–2281

[24] Fujiwara A, Watanabe S, Miyahara MT (2021) Flow microreactor synthesis of zeolitic imidazolate framework (ZIF)@ZIF core-shell metal-organic framework particles and their adsorption properties. Langmuir 37(13):3858–3867

[25] Tsao CS, Yu MS, Chung TY et al (2007) Characterization of pore structure in metal-organic framework by small-angle X-ray scattering. J Am Chem Soc 129(51):15997–16004

[26] Li YJ, Wang YL, Liu QY (2017) The highly connected MOFs constructed from nonanuclear and trinuclear lanthanide-carboxylate clusters: selective gas adsorption and luminescent pH Sensing. Inorg Chem 56(4):2159–2164

[27] Qin MH (2018) Lignocellulosic biomass refining, vol 6. Beijing Science Press, Bejing, p 88